

The cluster-core model for halo-structure of light nuclei at the drip lines.

Raj K. Gupta^{a,b}, Sushil Kumar^a, M. Balasubramaniam^{a,b}
G. Münzenberg^c and Werner Scheid^b,

^a *Physics Department, Panjab University, Chandigarh-160014, India.*

^b *Institut für Theoretische Physik, Justus-Liebig-Universität, Heinrich-Buff-Ring 16, D-35392, Giessen, Germany.*

^c *Gesellschaft für Schwerionenforschung mbH, Planckstrasse 1, D-64291 Darmstadt, Germany.*

Abstract

Nuclei at both the neutron- and proton-drip lines are studied. In the cluster-core model, the halo-structure of all the observed and proposed cases of neutron- or proton-halos is investigated in terms of simple potential energy surfaces calculated as the sum of binding energies, Coulomb repulsion, nuclear proximity attraction and the centrifugal potential for all the possible cluster+core configurations of a nucleus. The clusters of neutrons and protons are taken to be unbound, with additional Coulomb energy added for proton-clusters. The model predictions agree with the available experimental studies but show some differences with the nucleon separation energy hypothesis, particularly for proton-halo nuclei. Of particular interest are the halo-structures of ^{11}N and ^{20}Mg . The calculated potential energy surfaces are also useful to identify the new magic numbers and molecular structures in exotic nuclei. In particular, $N=6$ is a possible new magic number for very neutron-deficient nuclei, but $Z=N=2$ and $Z=8$ seem to remain magic even for such nuclei, near the drip line.

1 Introduction

The halo-structure refers to highly neutron-rich or proton-rich *light* nuclei that lie, respectively, near the neutron- or proton-drip line and hence are totally "unstable" systems. A number of such nuclei have now become available, both as the primary and secondary beams with various low, intermediate, and high energies, called the radioactive nuclear beams (RNBs). The structure properties of some of these nuclei are studied via the projectile fragmentation process in reactions using the intermediate and high energy RNBs. These structures are found to be different from the earlier known structures of nuclei at or near the β -stability line, and are referred to as halo or thick neutron (proton) skin structures, depending on the measurements made (see below). So far only 6-7 cases of neutron-halo and 3-4 cases of proton-halo nuclei are identified experimentally, but many more are proposed as the likely candidates. These are listed in Tables 1 and 2, respectively, for neutron- and proton-halo nuclei.

A halo or thick-skin nucleus is identified by its measured weak binding or small neutron (proton) separation energy, extended nucleon density distributions $\rho(r)$ (ρ_n for n-halo and ρ_p for p-halo, a model dependent property) or large root-mean-square radii (not following the $R = R_0 A^{\frac{1}{3}}$ law; for p-rich nuclei the enlargement of matter radii is observed to be not as much as for n-rich nuclei) and narrow momentum distributions of the emitted neutron(s) or proton(s) (observed to be more so for n-halo than for p-halo). The terminology thick neutron- or proton-skin is used when the nucleon density distribution is measured, representing the thickness of the extended neutron or proton surface. The other properties characterize these nuclei as halo nuclei which is more of an artistic view and is useful for developing a few-body theory (see below). Here, we note that the last two properties (extension in space and narrow momentum distribution of, say, neutrons) are related, since as an obvious consequence of the Heisenberg's uncertainty principle ($\Delta x \Delta p \sim \hbar$), a large extension in space must restrict the momentum to a narrow distribution. Apparently, the term halo or thick-skin serves for book keeping only. For the 1n and 2n separation energies defined, in terms of the binding energy $B(Z,N)$, as

$$S_{1n} = M(Z, N - 1) + M_n - M(Z, N) = B(Z, N) - B(Z, N - 1) \quad (1)$$

and

$$S_{2n} = B(Z, N) - B(Z, N - 2), \quad (2)$$

a nucleus is 1n- or 2n-halo nucleus if S_{1n} or S_{2n} is the lowest and is less than 1 MeV

(to be compared with 6–8 MeV for stable nuclei). The same is found to be nearly true for p-halo nuclei, i.e.

$$S_{1p} = M(Z - 1, N) + M_p - M(Z, N) = B(Z, N) - B(Z - 1, N) \quad (3)$$

or

$$S_{2p} = B(Z, N) - B(Z - 2, N), \quad (4)$$

is the lowest and less than 1 MeV, though the observed number of cases for p-halo are so far only a few. The 2n-halo nucleus is found to possess an additional characteristic property, namely: its isotope with one less neutron (for example, ^{10}Li for ^{11}Li) is also unbound [1]. Based on these characteristic properties, the experimentally observed 1n-halo nuclei are ^{11}Be and ^{19}C [2, 3, 4, 5] and the 2n-halo nuclei are $^{6,8}\text{He}$, ^{11}Li , ^{14}Be and ^{17}B [6, 7, 8, 9, 10]. Since the existence of a bound di-neutron in the ground-state is not yet observed [11, 12] (a free di-neutron is also unbound by about 70 KeV), apparently, we are dealing here with two-body (n+core) and three-body (n+n+core) structures, respectively, for the 1n- and 2n-halo nuclei. Table 1 shows that many other cases have been investigated, both theoretically and experimentally [13, 14, 15, 16, 17], and in some calculations [18] even a 3n-halo structure is predicted (for ^{26}F) which means a four-body system. Thus, it is evident that *a priori* information on the halo-structure of a nucleus is of vital importance for the theoretical treatment of these weakly bound nuclei as two-, three- or more-body problems [19]. Similar remarks apply to proton-halo nuclei, where 1p-halo structures are established for ^8B [20, 21] and ^{17}F [22] and the 2p-halo for only ^{17}Ne [22]. For ^{11}N , the experiments seem to indicate a 1p-halo structure [23], but in the following we find that this nucleus could be another case of a 4-body system (a 3p-halo structure). Table 2 shows many other experimental or theoretical possible cases [24, 25, 26], which includes even a possibility of the tetra-proton cluster surrounding the ^{16}O core proposed for ^{20}Mg [27].

The direct experimental information on the halo-structures of nuclei come from the Coulomb breakup studies or the nuclear dissociation mechanism (Coulomb dissociation of projectile in the presence of heavy targets) [4, 5, 9, 28]. The breakup process could either be a "direct process" or occur via a low energy (soft) dipole mode (a giant resonance phenomenon) between the core and skin- or halo-nucleons [29, 30], in addition to the normal dipole resonance where the neutron and proton cores are separated. However, the Coulomb dissociation experiments [31, 32] seem to rule out the possibility of a soft dipole resonance and suggest that the breakup of halo nuclei is a "direct

breakup” process. But, in a very recent charge exchange reaction ${}^6\text{Li}({}^7\text{Li}, {}^7\text{Be}){}^6\text{He}$ [33], a resonance is observed whose excitation energy, width and cross section seem consistent with those expected for a soft dipole resonance in ${}^6\text{He}$. On the other hand, the measured cross sections of an earlier charge changing reaction for ${}^{8,9,11}\text{Li}$ on C target strongly suggest that ${}^{11}\text{Li}$ is a three-body system with ${}^9\text{Li}$ as core and the two neutrons orbiting around it [34]. These results further strengthen the picture where the halo neutrons in, for example, ${}^{11}\text{Li}$ are taken to exist as unbound, rather than bound in a di-neutron. In other words, instead of a resonant state, an excited state of nonzero width is formed which has important consequences for the structure studies of neutron-rich nuclei [35, 36, 37].

In this paper, we dwell on the question of how to characterize, *a priori*, a nucleus as a halo-nucleus i.e. find the halo-structure of a nucleus. We discuss here a simple theoretical method of potential energy surfaces (PES), the cluster-core model (CCM), given recently by some of us [38, 39] for neutron-rich light nuclei. This was refereed to as (neutron) cluster-core model. We find that the method works equally well for proton-rich light nuclei, provided the Coulomb energy of protons in proton-clusters is added. This is now given the name (nucleon) cluster-core model; in short the CCM. Also, the new cases of possible neutron-halo are studied. It may be mentioned that this is the only known theoretical method for identifying the halo-structure of a n- or p-rich light nucleus, other than the hypothesis of (neutron or proton) separation energy described in the second paragraph above.

The (nucleon) cluster-core model (CCM) is described in section 2, with the results of our calculations for both the n- and p-halo nuclei presented in section 3. The possibility of identifying the newly arisen magic numbers in exotic nuclei, within the same cluster-core model, is also discussed in this section. A summary of our results is given in section 4.

2 The (nucleon) cluster-core model (CCM)

As already stated above, the CCM was first given [38, 39] for the neutron-clusters, and is now extended to proton-clusters also. Note that the cluster is now a general term, used not only for α -particle and heavier nuclei but also for one or two protons, since the proton-radioactivity is also understood on the basis of the models used for α -decay and exotic cluster radioactivity (see e.g. [40]). Here, we extend the same concept to neutron-clusters also, which seems to work equally well. In the CCM, we

calculate the potential energy surface (PES) of a nucleus for its all possible cluster-core (A_2, A_1) configurations and look for a neutron(s)-cluster (or proton(s)-cluster) + core configuration with a minimum potential energy, which in the language of the cluster-decay model (e.g. the Preformed Cluster Model of Gupta et. al. [41, 42, 43, 44]) means a configuration formed with the largest quantum mechanical probability. Such a picture is consistent with the model of Hansen and Jonson [45] where our cluster-core configuration could be understood as their quasi-deuteron picture of ^{11}Li , approximated as ^9Li core plus a di-neutron consisting of two *unbound* neutrons. Alternatively, our cluster-core configurations could be looked upon as few-body configurations of the type used in few-body theoretical calculations [19]. The calculated PES in CCM could also be used for the search of optimum molecular structures, reached in experiments via the break-up reactions [46].

The potential energy for a cluster-core configuration (A_2, A_1) of a nucleus A ($=A_1 + A_2$; A_1 and A_2 being, respectively, the core and cluster mass numbers) is defined simply as the sum of the two binding energies, the Coulomb repulsion, the additional attraction due to nuclear proximity and the rotational energy due to angular momentum:

$$V(A_1, A_2, R, \ell) = - \sum_{i=1}^2 B(A_i, Z_i) + \frac{Z_1 Z_2 e^2}{R} + V_P + V_\ell. \quad (5)$$

Here, $B(A_i, Z_i)$ are the experimental binding energies or mass excesses $\Delta m_A = M_A - A$ in energy units [47] (the two quantities differ through a constant since $M_A(Z, N) = ZM_p + NM_n - B(Z, N)$), V_P the nuclear proximity interaction energy [48] and V_ℓ the centrifugal potential [49] that pulls the fragments apart. The deformation effects are neglected here in both the Coulomb and proximity energies, for reasons of simplicity only. These effects are shown to be important for a complete quantitative cluster decay model calculation, specifically the cluster preformation probability [44]. Also, it may be pointed out that here we are using experimental binding energies and hence the microscopic shell effects are there in Eq. (5). However, it will be of interest to see the role of macroscopic liquid drop energy alone for the halo-structure. Like the α -nucleus structure in light-heavy nuclei is due to the Wigner term [50, 51], the halo-structure in light nuclei at the drip-lines could be due to the surface energy term in the liquid drop formula.

The charges Z_i in Eq. (5) are fixed by minimizing the sum of the two binding energies in Z_1 (or Z_2). Also, the shape of the potential $V(A_1, A_2, R, \ell)$ is known to be nearly independent of the choice of the value of R. This is shown explicitly in many

of our earlier publications (see e.g. in [52] for early works or in [53] for a review). Therefore, in view of our dealing here with light nuclei, we consider only touching configurations, i.e., $R = R_1 + R_2 = R_t$. In general, we define $R_i = R_0 A_i^{1/3}$, where R_0 has a constant value ($=1.15$ fm). This means that R_i depend only on A_i , i.e., $R_i(A_i)$. If we allow surface effects and define the Süssman central radius $C_i = R_i - (1/R_i)$, we still get $C_i = C_i(A_i)$. However, for halo nuclei R_0 changes considerably from nucleus to nucleus and from one isotope to another isotope. Therefore, we consider $R_0(Z_i, A_i)$ and take (or interpolate) its values for $Z \leq 10$ from the experimental [8, 22] or theoretical [54] data and for $Z > 10$ from the theoretical estimates of [24]. This means, we include the surface effects not only through Süssman central radii but also via the observed isotopic variations of the radii in halo nuclei. For the neutron radius, we approximate it to be the same as the root-mean-square (rms) radius of proton, namely 0.8 fm [22].

The binding energy for a cluster with x neutrons ($x \geq 1$) is taken to be x times that of the one-neutron binding energy (the mass excess $\Delta m_n = 8.0713$ MeV), i.e.

$$B(A_2 = xn) = x\Delta m_n. \quad (\text{for neutron-clusters}) \quad (6)$$

For proton-clusters, we define the same as

$$B(A_2 = xp) = x\Delta m_p - a_c A_2^{5/3}, \quad (\text{for proton-clusters}) \quad (7)$$

with $\Delta m_p = 7.2880$ MeV, the one-proton mass excess (equivalent of the one-proton binding energy), and $a_c = 0.7053$ MeV [55]. The additional term in (7) is the disruptive Coulomb energy ($= -a_c(Z_2^2/A_2^{1/3})$) between the x protons (here $x = A_2 = Z_2$). The above definitions for the binding energies of n- or p-clusters mean that the nucleons in these clusters are taken to be unbound, just as is the case in the model of Hansen and Jonson [45], the few-body theories [19] or as is suggested by the recent experiments [11, 12].

3 Calculations and results

We have calculated the potential energy surfaces $V(A_2)$ for all the neutron- and proton-rich nuclei listed in Tables 1 and 2, by using the experimental binding energies from the 1995 Tables of Audi and Wapstra [47] and $R_0 = R_0(Z_i, A_i)$ in $R_i = R_0 A_i^{1/3}$. Several of the n-halo nuclei listed in Table 1 were already studied in our earlier works [38, 39], and we discuss here the additional new cases proposed experimentally or theoretically. We find that all the nuclei considered here in Tables 1 and 2, except ^{11}N , are stable

($Q < 0$) against all possible cluster-core (A_2, A_1) configurations in the ground state. ^{11}N is unstable against all proton-cluster decays (such clusters are 1p-, 2p- and 3p-clusters). Also, the cluster-core configurations corresponding to the minima in these potential energy surfaces are the most probable cluster-core configurations formed for the cluster-decay process [41, 56], i.e., they occur with relatively larger preformation probabilities, compared to their neighbors. Of these cluster-core configurations, we are interested here only in the one(s) where a cluster of neutrons (or protons) is involved (the other configurations are also of interest, but more for seeking new magic numbers and molecular structures, etc.). Such a neutron(s) or proton(s) cluster will behave like a n- or p-halo since this is most loosely bound to the core. We find that the nuclei considered here are all either 1nucleon- or 2nucleon-halo nuclei, and we discuss them in the following separately for the two cases of n- and p-halo structures.

For the angular momentum part of the potential, we have considered both the cases of $\ell = 0$ and $\ell \neq 0$ ($\ell = 1, 2, 3$, chosen arbitrarily). In general, both the positions and depths of potential energy minima in $V(A_2)$ are *nearly* independent of the contribution of the ℓ -dependent term in the potential [49], but we find that in some cases, like for ^{11}N , ^{12}N and ^{24}O , there is a shift of the minimum to another nucleon-cluster. This point needs further investigation and perhaps refers to the mixed angular momentum and parity states for the ground state configuration [57, 58]. For this reason, in the following, we discuss only the $\ell = 0$ configurations.

3.1 Neutron-halo nuclei

Table 1 lists all the cases of neutron-halo studied here, as well as their one-neutron and two-neutron separation energies, S_{1n} and S_{2n} , the configurations with respect to the minimum in the PES calculated with the CCM and the N:Z ratios of the resulting core nuclei. The nuclei studied earlier in [39] are also included here in this table. We find that in agreement with our earlier results of [39], the cores could be classified mostly as the ones with $N=2Z$ and $2Z \pm 2$ nuclei. This means that nuclei with $2Z \pm 2$ are as stable as the $N = 2Z$ nuclei. The cores with $2Z - 3$ and $2Z - 4$ are also predicted by the CCM, but we notice in Table 1 that according to the neutron separation energy hypothesis, there is a question mark with the halo-structure of at least some of these nuclei (see footnotes in Table 1); e.g. for ^{22}O and ^{24}F both the neutron separation energies S_{1n} and S_{2n} are much larger than ~ 1 MeV. The halo nuclei with larger separation energies ($\gg 1$ MeV) are perhaps good cases of collective soft dipole excitations, though the

same is not realized experimentally as yet [59].

Figure 1 shows the results of our calculation for the four new cases, two each of 1n- and 2n-halo structures. We notice in Fig. 1 (upper frames) and Table 1 (upper part; for the corresponding PES of the earlier studied cases, see Fig. 1 in [39]) that for all the 1n-halo nuclei, the deepest minimum clearly occurs at the 1n+core configuration. The minimum in the PES means the most probable n-cluster+core configuration for the nucleus. Apparently, these nuclei can be considered as two-body (n+core) systems [19]. On the other hand, Table 1 shows that the neutron separation energy in all the 1n-halo nuclei is though minimum for S_{1n} , but is $\gg 1$ MeV for some cases (^{22}O , ^{23}O , ^{24}O and ^{24}F). These are, however, exotic nuclei, lying far from the β -stability line, and hence should be good candidates of halo structure [14, 18, 59, 60].

Figure 1 (lower frames) and Table 1 (lower part) show the results of our calculation for 2n-halo nuclei. In these nuclei, the neutron(s)-cluster minimum in the PES for each case is deepest at the 2n+core configuration and, except for ^{12}Be and ^{27}F , the S_{2n} is also the lowest. For both the ^{12}Be and ^{27}F , the lowest neutron separation energy is for one-neutron separation S_{1n} , whereas the PES for these nuclei show the 2n+core configuration lying clearly lowest (for ^{12}Be , also both S_{1n} and $S_{2n} \gg 1$ MeV). On the other hand, ^{29}F is clearly a 2n-halo nucleus from the point of view of the separation energy (S_{2n} is lowest, compared to S_{1n} and S_{3n}) but in the PES, the minima at 3n+ and 4n+core are almost as deep as for the 2n+core configuration (see Fig. 2 [39]). Hence, ^{29}F seems to be an isolated n-halo nucleus where neutron-clusters which are more complex than a di-neutron could exist, as was also expected by Migdal [61]. However, we have listed in Table 1 the ^{12}Be , ^{27}F and ^{29}F nuclei as 2n-halo nuclei from the point of view of the PES. Experimentally also, the ^{12}Be nucleus is expected [17] to have a 2n-halo structure, identical to that of the classical 2n-halo nucleus ^{11}Li . Another exception to the separation energy hypothesis is ^8He where both S_{1n} and $S_{2n} \gg 1$ MeV. This nucleus is now a well studied halo-nucleus [10] and is predicted to be a 2n-halo structure in the CCM. The other experimentally observed ^6He , ^{14}Be and ^{17}B are also the well studied structures of 2n-halo nuclei [6, 8, 9]. Three-body (n+n+core) calculations have also been made for some of these nuclei [19, 62, 63].

3.2 Proton-halo nuclei

Table 2 lists all the cases of 1p-, 2p- and possibly 3p-halo nuclei studied here. Figures 2 and 3 present the results of our calculation, respectively, for 1p- and 2p-halo nuclei.

^{11}N , the only case of predicted 3p-halo, is also included amongst the 1p-halo nuclei, since both experiments [23] and proton-separation energy hypothesis characterize it as a 1p-halo structure.

The proton-halo structures are so far observed only in a few cases (4 cases: 8B , ^{11}N , ^{17}F and ^{17}Ne), because of the suppression of the p-halo cluster minimum in PES by the Coulomb forces; the Coulomb repulsion is zero for neutrons and hence the n-halo configurations lie lower. Once again we discuss here only the case of $\ell = 0$, since the ℓ -contribution to both the positions and relative depths of potential energy minima is found small, except for the two $^{11,12}N$ nuclei (see Fig. 2).

Table 2 and Fig. 2 (excluding the ^{11}N nucleus) show that for all the 1p-halo nuclei, the results of our CCM calculation (the PES minima) agree completely with those of the S_{1p} hypothesis. This includes the two observed cases of 8B and ^{17}F [20, 22] and the three experimentally or theoretically proposed cases of ^{12}N , ^{26}P and ^{27}P [13, 24, 25]. The theoretical predictions are based on the shell model [24] and RMF [25] calculations. For the 2p-halo nuclei, however, our theoretical method of PES disagrees with the proton separation energy hypothesis in more than one way. For 9C , ^{18}Ne and ^{27}S , whereas the proton-separation energy in Table 2 is the lowest for S_{1p} , the PES in Fig. 3 show clear minima at 2p+core configurations. The shell model [24] and RMF [26] calculations also predict both the ^{18}Ne and ^{27}S to be the 2p-halo nuclei. Also, for ^{18}Ne (and so also for ^{20}Mg) both S_{1p} and S_{2p} are $\gg 1$ MeV. The ^{20}Mg nucleus, which is a 2p-halo structure on the basis of the PES (Fig. 3), is a case of special interest. This is predicted as 4 protons circulating the ^{16}O core on the basis of Coulomb displacement energies [27]. The CCM calculations show that the 4p+core configuration is also one of the possible configurations in $V(\eta_Z)$ (see inset, Fig. 3, ^{20}Mg) but is not the most preferred one (does not lie at the minimum either in $V(\eta_Z)$ or in $V(A_2)$). Also, the RMF calculations for ^{20}Mg [26] support the 2p-halo configuration, as is predicted by the CCM.

The ^{11}N nucleus is listed in Table 2 as a 1p- or 3p-halo structure. This is a completely unstable nucleus against proton-decays, since $Q > 0$ for its 1p-, 2p- and 3p-decays. The S_{1p} is negative and lowest which means that it is a 1p-halo nucleus according to the proton-separation energy hypothesis. The experimental observation of its ground state and excitation spectra also give it a 1p-halo configuration [23]. However, the PES in Fig. 3 present it as a clear 3p-halo structure. Apparently, further measurements and calculations are essential, since as per present calculations this nucleus seems to be the first candidate of a rather more complex p-halo structure.

Finally, the core configurations for p-halo nuclei consist of $Z=N$ or $Z=N+1$, which means that $Z=N+1$ core is as stable as the $Z=N$ one. Also, cores with $Z=N+2$ and $N+3$ are predicted but these are the cases where the halo structure is still to be confirmed experimentally.

3.3 New magic numbers in exotic nuclei

We consider here only the case of ^{20}Mg , as an illustrative example, and show that $N=6$ arises as a magic number for the very neutron-deficient, exotic nuclei only.

We know that in a potential energy surface, like the ones shown in Figs. 1-3, the minima arise only due to the shell effects of either one or both the fragments [53, 56]. This means that at the potential energy minima, at least one of the contributing nucleus must be a magic or nearly magic nucleus. In Fig. 3, the calculated PES for ^{20}Mg gives four minima, where both the participating nuclei are shown. We notice that for the very neutron-deficient nuclei near the drip-line, like ^{16}Ne and ^{14}O , $N=6$ could be the magic number but for the neutron-deficient nuclei, like ^{18}Ne , lying not too far from the β -stability line, $N=8$ is still the magic number. The $N=2$ and $Z=2$ magicities seem to be kept as such for both the classes (near and far away from β -stability line) of nuclei. Also, $Z=8$ seems to remain magic for both kinds of nuclei, since the proton numbers combining with all the $N=6$ (or its neighboring) nuclei are with $Z=8$ or its neighbors with $Z=8\pm 2$. This is an interesting result and needs further investigations on the basis of the CCM as well as other methods [60, 64, 65].

4 Summary

Summarizing, we have extended the cluster-core model (CCM), given by some of us [38, 39] earlier for (unbound) neutron-clusters, to include also the (unbound) proton-clusters. In other words, the cluster-core model could now be used to find, a priori, the halo-structure of any light nucleus approaching the β^+ - or β^- -instability, i.e., the light neutron- and proton-rich nuclei near the neutron- and proton-drip lines. This knowledge is important for building any few-body theory of these weakly bound systems. The CCM is applied to all known cases, experimentally established and/or theoretically proposed as the likely candidates, of neutron- and proton-halos. For proton-halo nuclei, an additional Coulomb energy is found essential for the, otherwise unbound, proton-clusters. In comparison to the only other known hypothesis of neutron (or

proton) separation energy, the present model works well without any exception. A theoretical method is in any case preferred over an (empirical) hypothesis and this is the merit of the CCM presented here. The predictions of the two methods (CCM and nucleon separation energy hypothesis) differ in many cases and this is more so for proton-halo nuclei. One such interesting case is of 3p-halo structure predicted by the CCM for a completely proton-unbound ^{11}N nucleus. ^{20}Mg is perhaps another interesting nucleus where both S_{1p} and S_{2p} are $\gg 1$ MeV and the CCM predicts it to be a 2p-halo structure in contradiction to its expected $4p + {}^{16}\text{O}$ configuration.

The calculated potential energy surfaces (PES) in CCM are also useful for searching the possible new magic numbers and optimum molecular structures for exotic nuclei. Our first analysis of the PES for ^{20}Mg nucleus allows us to identify $N=6$ as the possible magic number for very neutron-deficient nuclei near the drip line, though $N=8$ is still shown to be a magic number for neutron-deficient nuclei not too far from the line of β -stability. Also, $Z=N=2$ and $Z=8$ are found to remain magic even for very neutron-deficient nuclei.

Acknowledgments:

RKG, MB and WS are thankful to Volkswagen-Stiftung, Germany, for the support of this research work under a Collaborative Reserach Project between the Panjab University and Giessen University. RKG and MB are also thankful to the Council of Scientific and Industrial Research (CSIR), New Delhi, for the partial support of this research work. SK is thankful to Department of Atomic Energy (DAE), Govt. of India for a Junior Research Fellowship.

References

- [1] B.M. Young, et al., Phys. Rev. **C 49**, 279 (1994).
- [2] R. Anne, et al., Phys. Lett. **B 304**, 55 (1993).
- [3] J.H. Kelley, et al., Phys. Rev. Lett. **74**, 30 (1995).
- [4] F.M. Marques, et al., Phys. Lett. **B 381**, 407 (1996).
- [5] D. Bazin, et al., Phys. Rev. Lett. **74** (1995) 3569; Phys. Rev. **C 57**, 2156 (1998).
- [6] I. Tanihata, et al., Phys. Lett. **160 B**, 380 (1985); Phys. Rev. Lett., **55**, 2676 (1985).
- [7] I. Tanihata, et. al., Phys. Lett. **B 289**, 261 (1992).
- [8] M.G. Saint-Laurent, et al., Z. Phys. **A 332**, 457 (1989).
- [9] N.A. Orr, et al., Phys. Rev. **C 51**, 3116 (1995).
- [10] G.D. Alkhalaf, et al., Phys. Rev. Lett., **78**, 2313 (1997).
- [11] K. Ieki, et al., Phys. Rev. **C 54**, 1589 (1996).
- [12] E. Sauvan, et al., Phys. Rev. Lett., **87**, 042501 (2001).
- [13] I. Tanihata, Prog. Part. Phys. Nucl. Phys. **35**, 505 (1995); J. Phys. G: Nucl. Part. Phys. **22**, 157 (1996).
- [14] A.C.C. Villari, et. al. Phys. Lett. **B 268**, 345 (1991).
- [15] P.G. Hansen, et. al., Ann. Rev. Nucl. Part. Phys. **45**, 591 (1995).
- [16] U.C. Bergmann, et al., Eur. Phys. J. A **11**, 279 (2001).
- [17] A. Navin, et al., Phys. Rev. Lett., **85**, 266 (2000).
- [18] Z. Ren, B. Chen, Z. Ma, Z. Zhu and G. Xu, J. Phys. G: Nucl. Part. Phys. **22**, 523 (1996).
- [19] I.J. Thompson and J.S. Vaagen, in *Heavy Elements and Related New Phenomena*, Vol. II, Editors: W. Greiner and R.K. Gupta, World Sc., Singapore, 1999, p. 976.

- [20] W. Schwab, et al., Z. Phys. **A 350**, 283 (1995).
- [21] V. Guimarães, et al., Phys. Rev. Lett., **84**, 1862 (2000).
- [22] A. Ozawa, et al., Phys. Lett. **B 334**, 18 (1994).
- [23] J.M. Oliveira, Jr., et al., Phys. Rev. Lett., **84**, 4056 (2000).
- [24] B.A. Brown and P.G. Hansen, Phys. Lett. **B 381**, 391 (1996).
- [25] Z. Ren, B. Chen, Z. Ma and G. Xu, Phys. Rev. **C 53**, R572 (1996).
- [26] Z. Ren, W. Mittig, B. Chen, Z. Ma and G. Auger, Z. Phys. **A 353**, 363 (1996).
- [27] L. Chulkov, E. Roeckl and G. Kraus, Z. Phys. **A 353**, 351 (1996).
- [28] M. Labiche, et al., Phys. Rev. Lett., **86**, 600 (2001).
- [29] N. Takigawa and H. Sagawa, Phys. Lett. **B 265**, 23 (1991).
- [30] C.H. Dasso and R. Donangelo, Phys. Lett. **B 276**, 1 (1992).
- [31] D. Sackett, et. al., Phys. Rev. **C 48**, 118 (1993).
- [32] T. Nakamura, et. al., Phys. Lett. **B 331**, 296 (1994).
- [33] S. Nakayama, et al., Phys. Rev. Lett., **85**, 262 (2000).
- [34] B. Blank, et al. Z. Phys. **A 343**, 375 (1992).
- [35] A. Csóto, Phys. Rev. **C 49**, 3035 (1994)
- [36] M.V. Zhukov, A.A. Korshennikov and M.H. Smedberg, Phys. Rev. **C 50**, R1 (1994).
- [37] H. Esbensen, G.F. Bertsch and K. Ieki, Phys. Rev. **C 48**, 326 (1993).
- [38] R.K. Gupta, S. Kumar and W. Scheid, J. Phys. G: Nucl. Part. Phys. **21**, L27 (1995).
- [39] R.K. Gupta, M. Balasubramaniam, R.K. Puri and W. Scheid, J. Phys. G: Nucl. Part. Phys. **26**, L23 (2000).
- [40] B. Buck, A.C. Merchant and S.M. Perez, Phys. Rev. **C 45**, 1688 (1992).

- [41] R.K. Gupta, in *Proceedings of the 5th International Conference on Nuclear Reaction Mechanisms*, Varenna, Italy (1988), Editor: E. Gadioli, Ricerca Scientifica ed Educazione Permanente, Milano, 1988, p. 416.
- [42] S. S. Malik and R.K. Gupta, *Phys. Rev. C* **39**, 1992 (1989).
- [43] R.K. Gupta, W. Scheid and W. Greiner, *J. Phys. G: Nucl. Part. Phys.* **17**, 1731 (1991).
- [44] S. Kumar and R.K. Gupta, *Phys. Rev. C* **55**, 218 (1997).
- [45] P.G. Hansen and B. Jonson, *Europhys. Lett.* **4**, 409 (1987).
- [46] P.J. Leask, et al., *J. Phys. G: Nucl. Part. Phys.* **27**, B9 (2001).
- [47] G. Audi and A.H. Wapstra, *Nucl. Phys. A* **595**, 4 (1995).
- [48] J. Blocki, J. Randrup, W.J. Swiatecki and C.F. Tsang, *Ann. Phys. (NY)* **105**, 427 (1977).
- [49] D.R. Saroha, N. Malhotra and R.K. Gupta, *J. Phys. G: Nucl. Phys.* **11**, L27 (1985).
- [50] M.K. Sharma, R.K. Gupta and W. Scheid, *J. Phys. G: Nucl. Part. Phys.* **26**, L45 (2000).
- [51] R.K. Gupta, M. Balasubramaniam, C. Mazzocchi, M. La Commara and W. Scheid, *Phys. Rev. C* **65**, 024601 (2002).
- [52] A. Săndulescu, R.K. Gupta, W. Scheid and W. Greiner, *Phys. Lett.* **60 B**, 225 (1976); R.K. Gupta, *Z. Physik A* **281**, 159 (1977); *Phys. Rev. C* **21**, 1278 (1980).
- [53] R.K. Gupta and W. Greiner, in *Heavy Elements and Related New Phenomena*, Vol. I, Editors: W. Greiner and R.K. Gupta, World Sc., Singapore, 1999, p. 397.
- [54] F. Grümmer, B.Q. Chen, Z.Y. Ma and S. Krewald, *Phys. Lett. B* **387**, 673 (1996).
- [55] W. Myers and W.J. Swiatecki, *Nucl. Phys.* **81**, 1 (1966)
- [56] R.K. Gupta, in *Heavy Elements and Related New Phenomena*, Vol. II, Editors: W. Greiner and R.K. Gupta, World Sc., Singapore, 1999, p. 730.

- [57] H. Simon, et al., Phys. Rev. Lett., **83**, 496 (1999).
- [58] U. Datta Pramanik, et al., GSI Scientific Report 2000, Report no. 2001-1, p.23.
- [59] A. Leistenschneider, et al., Phys. Rev. Lett., **86**, 5442 (2001).
- [60] A. Ozawa, T. Kobayashi, T. Suzuki, K. Yoshida, and I. Tanihata, Phys. Rev. Lett., **84**, 5493 (2000).
- [61] A.B. Migdal, Sov. J. Nucl. Phys. **16**, 238 (1973).
- [62] E. Garrido and E. Moya de Guerra, Nucl. Phys. **A 650**, 387 (1999).
- [63] K. Arai, Y. Suzuki and R.G. Lovas, Phys. Rev. **C 59**, 1432 (1999).
- [64] T. Otsuka, R. Fujimoto, Y. Utsuno, B.A. Brown, M.Honma, and T. Mizusaki, Phys. Rev. Lett., **87**, 082502 (2001).
- [65] B.K. Raj, S.K. Patra and R.K. Gupta, to be published.

Figure Captions

Fig. 1 The potential energy V as a function of the light cluster mass A_2 for 1n- and 2n-halo nuclei, showing the deepest minimum at 1n- (or 2n-) cluster + core configurations. For $R_0(Z_i, A_i)$, see text.

Fig. 2 The same as for Fig. 1, but for 1p- and 3p-halo nuclei, showing the deepest minimum at 1p (or 3p)-cluster+core configurations. The 3p-cluster+core configuration is predicted only for ^{11}N nucleus.

Fig. 3 The same as for Fig. 2, but for 2p-halo nuclei, showing the deepest minimum at 2p-cluster + core configurations.

Table 1: The calculated halo-characteristics of light neutron-rich nuclei. The neutron separation energies are calculated by using the binding energy tables of [47] and the configurations resulting from the potential energy surfaces (PES) are with respect to the $\ell = 0$ case. For observed cases, see text.

Structure	Nucleus	S_{1n} (KeV)	S_{2n} (KeV)	PES Minimum (Cluster+core Config.)	Core (N:Z)
1n-halo	^{11}Be	504	7317	$1n + ^{10}\text{Be}$	N=2Z-2
	^{14}B	970	5848	$1n + ^{13}\text{B}$	N=2Z-2
	^{15}C	1218	9394	$1n + ^{14}\text{C}$	N=2Z-4
	^{17}C	729	4979	$1n + ^{16}\text{C}$	N=2Z-2
	^{19}C	162	4346	$1n + ^{18}\text{C}$	N=2Z
	^{22}N	1222	5828	$1n + ^{21}\text{N}$	N=2Z
	^{22}O	6848*	10655	$1n + ^{21}\text{O}$	N=2Z-3
	^{23}O	2740*	9588	$1n + ^{22}\text{O}$	N=2Z-2
	^{24}O	3713*	6453	$1n + ^{23}\text{O}$	N=2Z-1
	^{24}F	3857*	11392	$1n + ^{23}\text{F}$	N=2Z-4
	^{26}F	1050	5399	$1n + ^{25}\text{F}$	N=2Z-2
	^{29}Ne	1330	5216	$1n + ^{28}\text{Ne}$	N=2Z-2
2n-halo	^6He	1864	974	$2n + ^4\text{He}$	N=2Z-2
	^8He	2583*	2138	$2n + ^6\text{He}$	N=2Z
	^{11}Li	326	301	$2n + ^9\text{Li}$	N=2Z
	^{12}Be	3169*, ^a	3673	$2n + ^{10}\text{Be}$	N=2Z-2
	^{14}Be	1847	1336	$2n + ^{12}\text{Be}$	N=2Z
	^{17}B	1437	1393	$2n + ^{15}\text{B}$	N=2Z
	^{19}B	1029	495	$2n + ^{17}\text{B}$	N=2Z+2
	^{22}C	1448	1120	$2n + ^{20}\text{C}$	N=2Z+2
	^{27}F	1309 ^a	2359	$2n + ^{25}\text{F}$	N=2Z-2
	$^{29}\text{F}^b$	1002	897	$2n + ^{27}\text{F}$	N=2Z

* Note that the neutron separation S_{1n} (or S_{2n}) is much larger than ~ 1 MeV.

^a The S_{1n} -value is lower than the S_{2n} -value, whereas in the PES the 2n minimum is clearly the lowest.

^b The S_{2n} -value is lower and the minimum in PES also lies at 2n+core configuration, though in the PES, for both $\ell = 0$ and $\ell \neq 0$ cases, the 2n, 3n and 4n minima are very close to each other. However, the S_{3n} -value (2206 KeV) is higher than both the S_{1n} and S_{2n} energies.

Table 2: Same as for Table 1, but for proton-rich nuclei.

Structure	Nucleus	S_{1p} (KeV)	S_{2p} (KeV)	PES Minimum (Cluster+Core Config.)	Core (N:Z)
1p-halo	8B	137	5743	$1p + {}^7Be$	Z=N+1
	${}^{12}N$	601	9290	$1p + {}^{11}C$	Z=N+1
	${}^{17}F$	600	12727	$1p + {}^{16}O$	Z=N
	${}^{26}P$	141	3549	$1p + {}^{25}Si$	Z=N+3
	${}^{27}P$	897	6415	$1p + {}^{26}Si$	Z=N+2
2p-halo	9C	1296 ^a	1433	$2p + {}^7Be$	Z=N+1
	${}^{17}Ne$	1484	948	$2p + {}^{15}O$	Z=N+1
	${}^{18}Ne$	3932 ^b	4534	$2p + {}^{16}O$	Z=N+1
	${}^{20}Mg$	2647 ^b	2314	$2p + {}^{18}Ne$	Z=N+2
	${}^{27}S$	755 ^a	896	$2p + {}^{25}Si$	Z=N+3
1p/3p-halo	${}^{11}N$	-1973*	2033	$3p + {}^8Be$	Z=N

* Note that here S_{1p} is negative, which means a completely unstable system against 1p-decay (Q_{1p} -value=1.974 MeV). However, the PES prefers a 3p-halo and it is also unstable against 3p-decay (Q_{3p} -value=2.556 MeV). Also, it is unstable against 2p-decay (Q_{2p} -value=0.208 MeV). Furthermore, S_{3p} =1.848 MeV, which means $S_{3p} < S_{2p}$.

^a Though $S_{1p} < S_{2p}$, the PES suggests this nucleus as 2p-halo.

^b Both S_{1p} and S_{2p} are $\gg 1$ MeV.

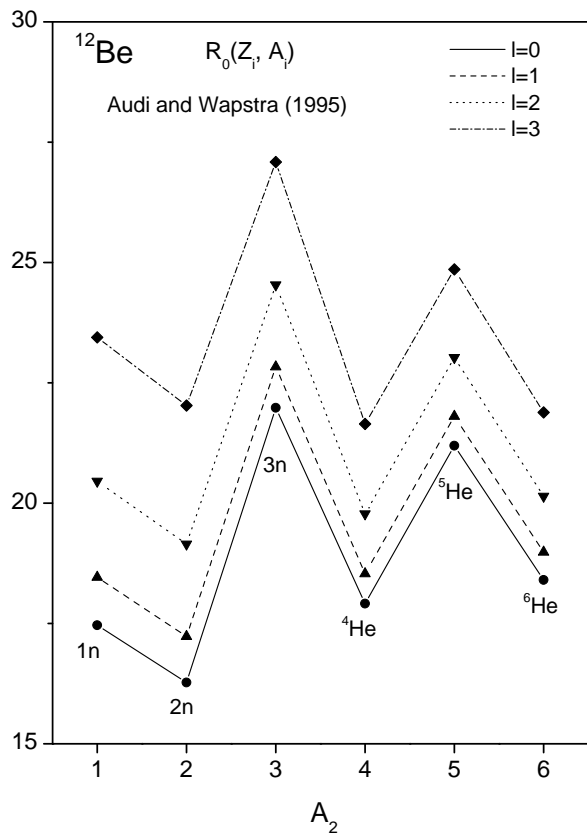
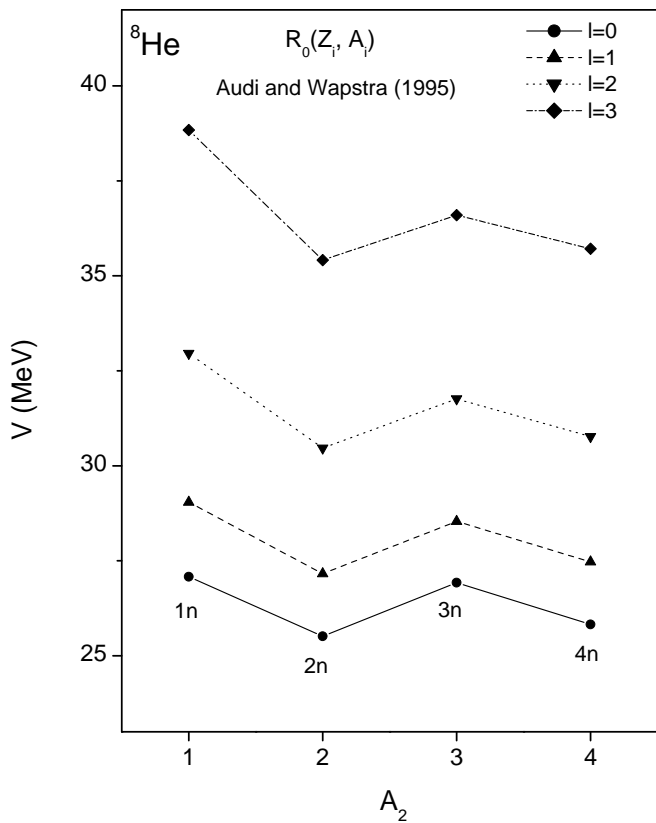
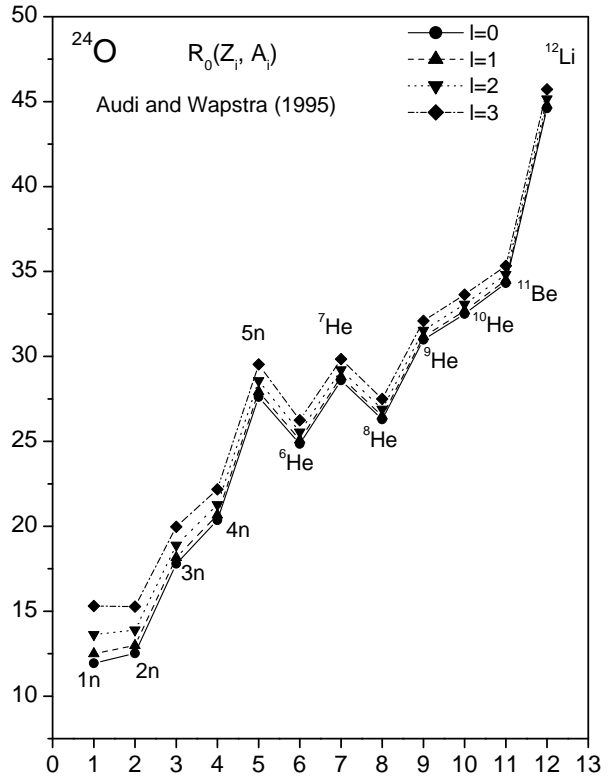
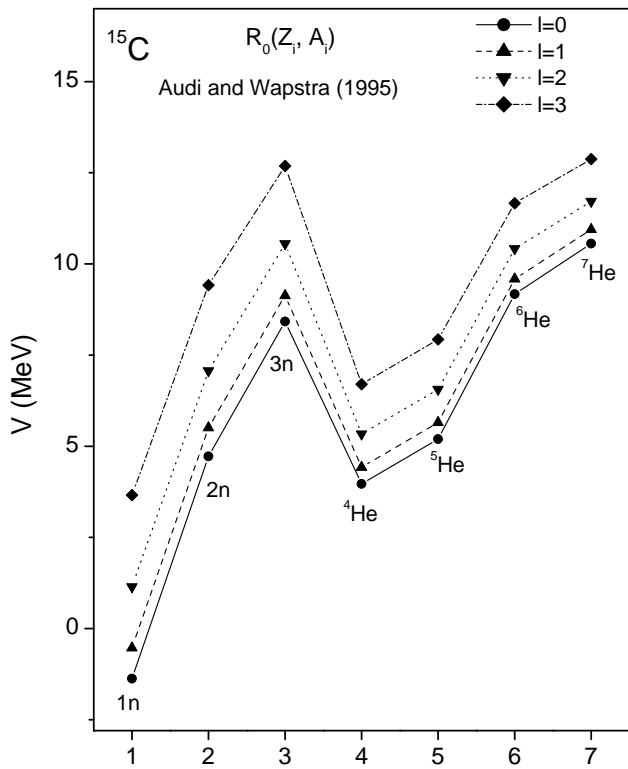


Fig. 1

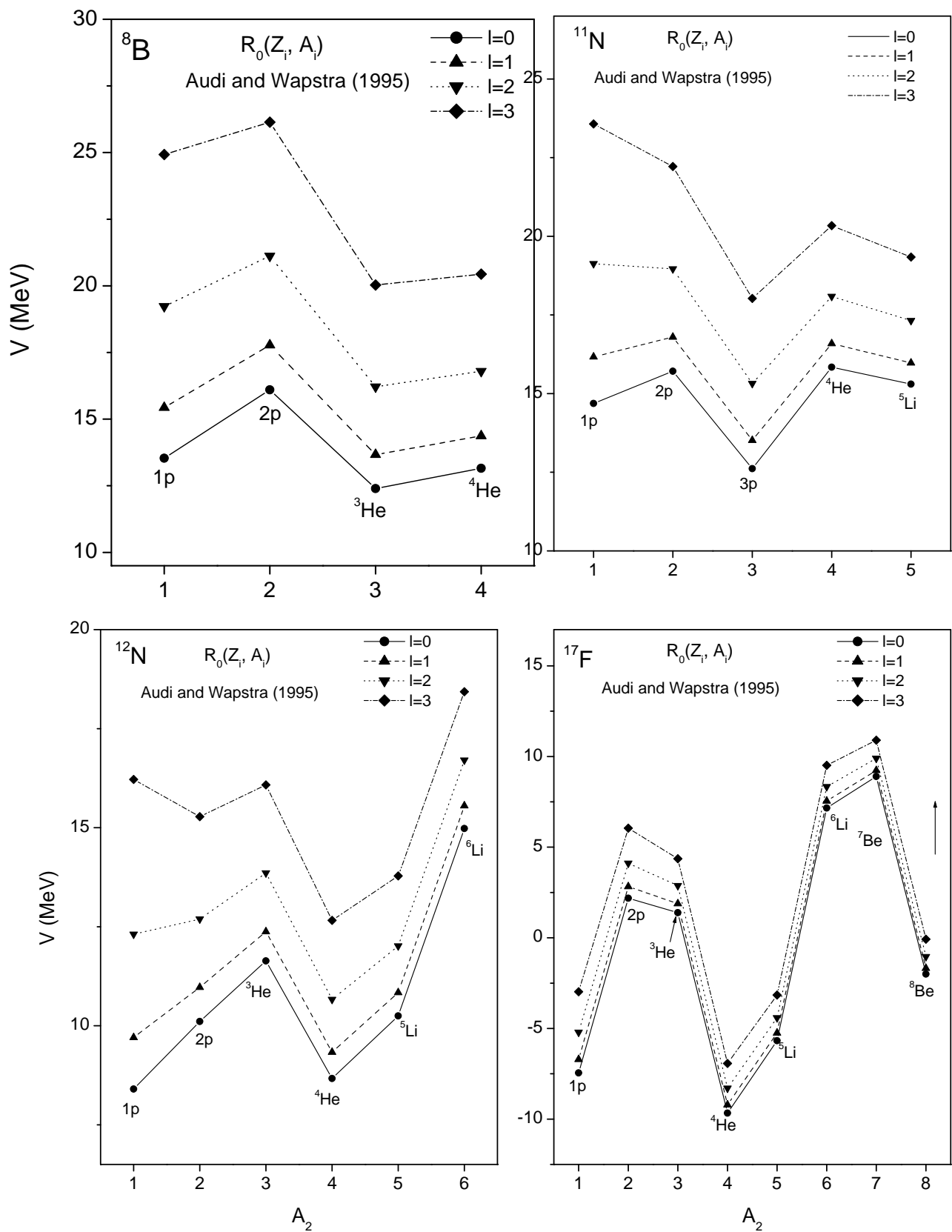


Fig. 2

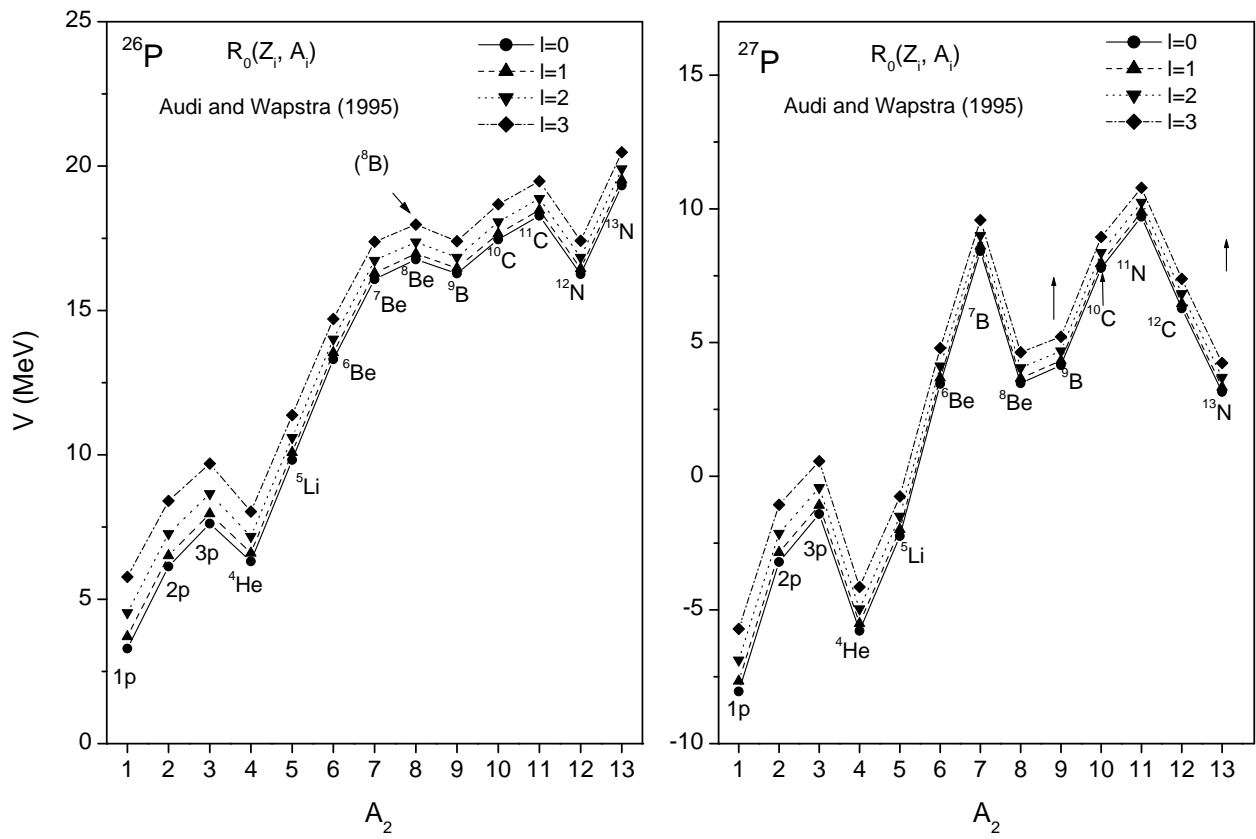


Fig. 2 - Continued

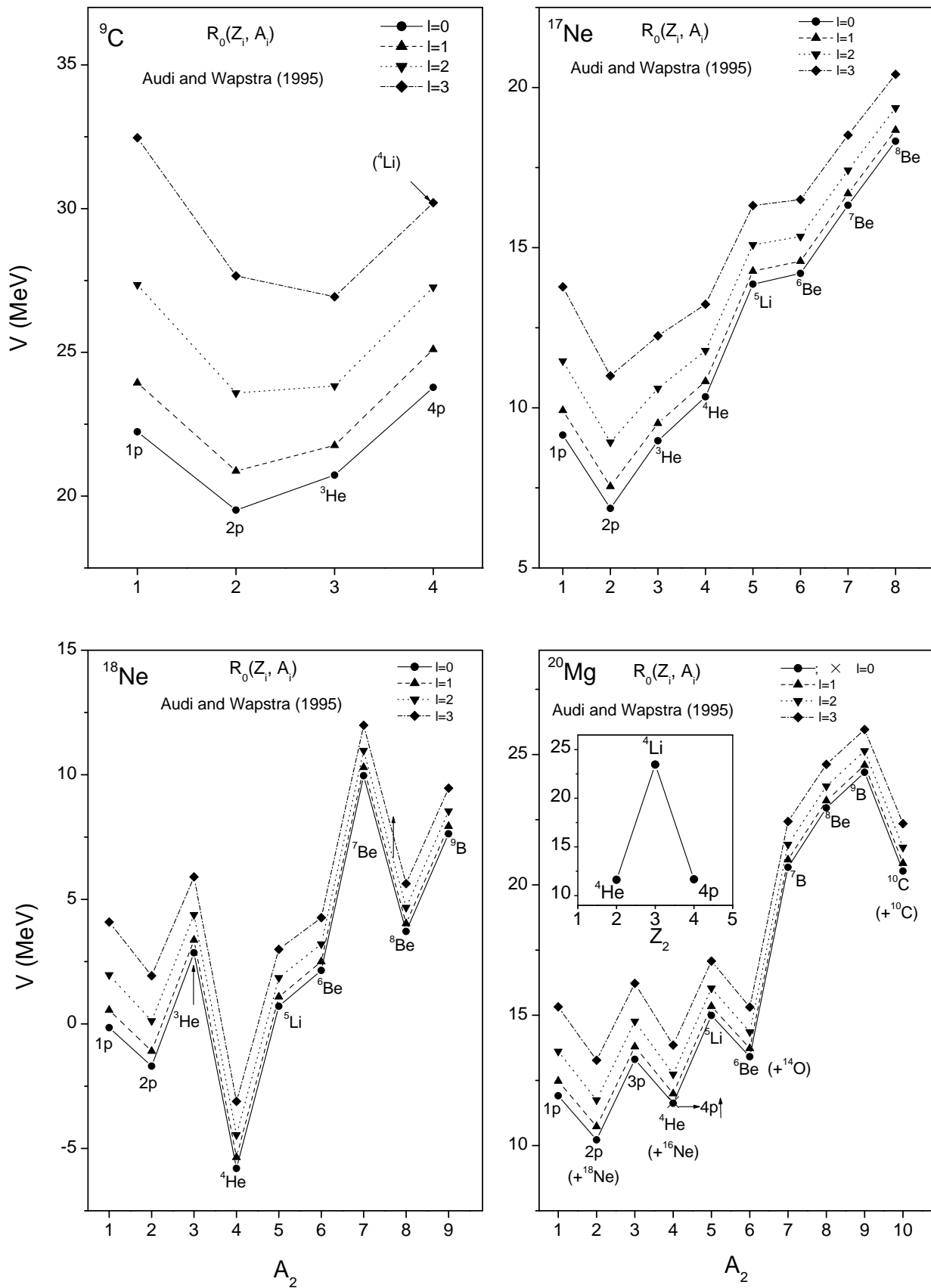


Fig. 3

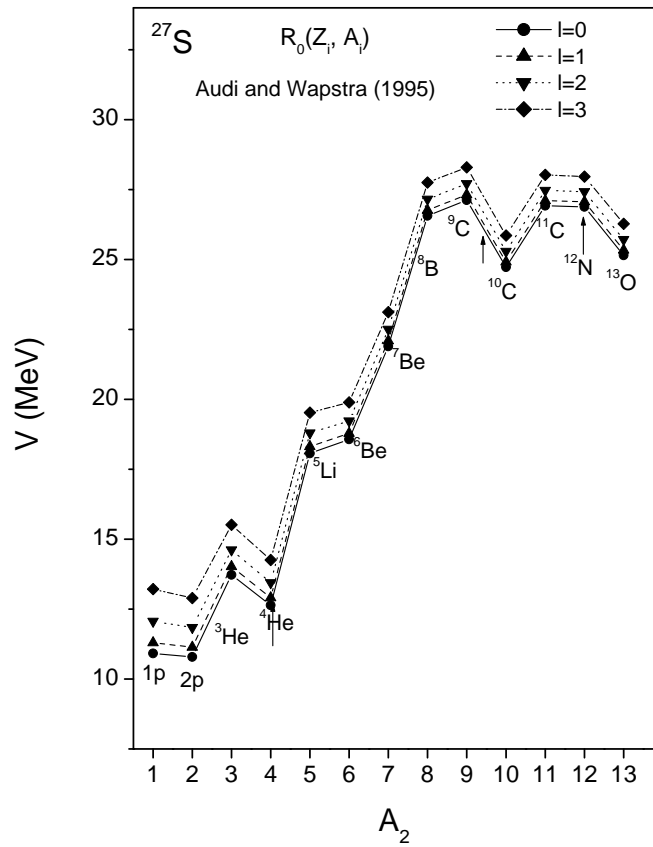


Fig. 3 - Continued